

# Fabrication of Conjugated Polymer Nanowires by Edge Lithography

Darren J. Lipomi, Ryan C. Chiechi, Michael D. Dickey, and George M. Whitesides\*

Department of Chemistry and Chemical Biology, Harvard University, 12 Oxford Street, Cambridge, Massachusetts 02138

Received April 2, 2008; Revised Manuscript Received May 8, 2008

## ABSTRACT

This paper describes the fabrication of conjugated polymer nanowires by a three stage process: (i) spin-coating a composite film comprising alternating layers of a conjugated polymer and a sacrificial material, (ii) embedding the film in an epoxy matrix and sectioning it with an ultramicrotome (nanoskiving), and (iii) etching the sacrificial material to reveal nanowires of the conjugated polymer. A free-standing, 100-layer film of two conjugated polymers was spin-coated from orthogonal solvents: poly(2-methoxy-5-(2'-ethylhexyloxy)-1,4-phenylenevinylene) (MEH-PPV) from chloroform and poly(benzimidazobenzophenanthroline ladder) (BBL) from methanesulfonic acid. After sectioning the multilayer film, dissolution of the BBL with methanesulfonic acid yielded uniaxially aligned MEH-PPV nanowires with rectangular cross sections, and etching MEH-PPV with an oxygen plasma yielded BBL nanowires. The conductivity of MEH-PPV nanowires changed rapidly and reversibly by  $>10^3$  upon exposure to  $I_2$  vapor. The result suggests that this technique could be used to fabricate high-surface-area structures of conducting organic nanowires for possible applications in sensing and in other fields where a high surface area in a small volume is desirable.

We have developed a method for the fabrication of electrically conductive nanowires of two conjugated polymers—poly(2-methoxy-5-(2'-ethylhexyloxy)-1,4-phenylenevinylene) (MEH-PPV) and poly(benzimidazobenzophenanthroline ladder) (BBL)—by sectioning spin-coated multilayer films with an ultramicrotome (“nanoskiving”, see Figure 1 for chemical structures).<sup>1-5</sup> We measured conductivity through groups of 50 to several hundred of these nanowires, which can have cross sectional widths and heights of  $\sim 100$  nm, over distances as long as  $100 \mu\text{m}$ . Polymer nanowires are versatile structures that are sensitive chemical<sup>6,7</sup> and biological<sup>8</sup> sensors, field-effect transistors,<sup>9-11</sup> interconnects in electronic circuitry,<sup>12</sup> and tools for studying one-dimensional charge transport in materials.<sup>13</sup> Of the methods available for the fabrication of conjugated polymer nanowires, most are specific to certain combinations of materials and substrates, and many require expensive or specialized equipment.<sup>9</sup> With the goal of developing inexpensive and simple methodology for nanofabrication, we have developed a technique for the fabrication of conjugated polymer nanowires that requires only a spin-coater and an ultramicrotome; the only requirement of the conjugated polymers is that they form thin films. After sectioning, the nanowires remain embedded in a macroscopic slab of embedding epoxy, which can be positioned manually on a desired substrate.

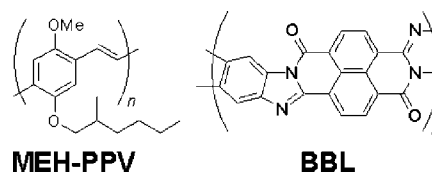


Figure 1. Chemical structures of MEH-PPV and BBL.

Amorphous organic semiconductors such as conjugated polymers possess many of the useful electrical properties of traditional crystalline semiconductors (most importantly, electroluminescence,<sup>14</sup> photovoltaic response,<sup>15</sup> and modulation of conductivity by gate voltage<sup>16</sup> or by doping<sup>17</sup>). Polymers are more mechanically flexible and less expensive to produce and process than crystalline semiconductor materials. As a result, there is a vast literature devoted to the fabrication and patterning of functional conjugated polymer structures.<sup>18</sup> One of the simplest and most useful small-dimensional geometries is the nanowire.<sup>9,19</sup>

Nanowires composed of conjugated polymers are well-suited for chemical sensing because they have a high ratio of area to volume; this feature permits rapid diffusion of an analyte into and out of a wire (or adsorption/desorption from its surface).<sup>6,20</sup> These characteristics allow electrical response and recovery rates that are superior to those of devices based on thin films or fibrous networks. Incorporation of molecular recognition elements into conjugated polymer nanowires is relatively straightforward by synthesis; analogous modifications of carbon nanotubes and inorganic nanowires require

\* Corresponding author. Telephone: (617) 495-9430. Fax: (617) 495-9857. E-Mail: gwhitesides@gmgroup.harvard.edu.

surface reaction(s) carried out postfabrication.<sup>8</sup> Other possible uses for conjugated polymer nanowires are as tools for studying one-dimensional charge transport<sup>21</sup> or as field-effect transistors,<sup>11</sup> actuators,<sup>22</sup> or interconnects.<sup>12</sup>

Despite the growing interest in conjugated polymer nanowires, there is not yet a truly general technique for the fabrication of these structures. Two of the most versatile techniques for the fabrication of conjugated polymer nanowires are templated electrodeposition and electrospinning. Penner and co-workers have developed a technique of electrodeposition in a template that can produce electrically addressable nanowires confined to trenches,<sup>23</sup> but it requires electron-beam lithography, is limited to materials that polymerize in situ, and is only compatible with rigid substrates, to which the nanowires are permanently attached. Craighead and co-workers have used scanned electrospinning<sup>24</sup> to deposit single nanowires of polyaniline<sup>6</sup> and poly(3-hexylthiophene)<sup>11</sup> on a rotating substrate, while Xia and co-workers have developed an approach to deposit uniaxial collections of nanofibers of a range of inorganic and organic materials.<sup>25,26</sup> Processes involving two or more techniques in combination have also been reported: Chi et al. have patterned high-density arrays of polypyrrole and polyaniline by a process comprising electron-beam and nanoimprint lithographies.<sup>27</sup> Lastly, dip-pen nanolithography, a versatile tool created by the Mirkin Laboratory, has been shown to form nanowires of charged conjugated polymers.<sup>28</sup>

**Nanoskiving.** We have developed a technique, nanoskiving, for fabricating nanostructures by sectioning patterned or stacked thin films of inorganic materials with an ultramicrotome.<sup>4</sup> It is a form of edge lithography: the ultramicrotome exposes the cross section of an embedded thin film to form the lateral dimension of a nanostructure.<sup>29</sup> The technique is amenable to conjugated polymers because most of these materials (i) form thin films (by spin-coating), (ii) are tough enough to be sectioned by a diamond knife without fracture, and (iii) adhere to the embedding matrix (usually epoxy). The nanostructures, after sectioning, remain embedded in a thin slab of the epoxy matrix. The slab is a flexible macroscopic object (mm<sup>2</sup> range) that one can manipulate and position/orient on a substrate containing, for example, patterned electrodes. The combination of forming thin films and nanoskiving can create structures with high aspect ratios and cross-sectional dimensions of 100 nm or less.

**Choice of Polymers.** The goal of this work was to form nanowires of conjugated polymers by sectioning spin-coated films with an ultramicrotome. We reasoned that we could fabricate multiple nanowires in this way by spin-coating a composite film of two or more polymers, in which every other layer would be a sacrificial material that we could remove from the final structure (see Figure 2 for an overview).

We explored two polymers, poly(2-methoxy-5-(2'-ethylhexyloxy)-1,4-phenylenevinylene) (MEH-PPV) and poly(benzimidazobenzophenanthroline ladder) (BBL); these polymers have different properties and are processed in different ways. MEH-PPV is a "p-type", solution-processible conjugated polymer that is soluble in organic solvents (including

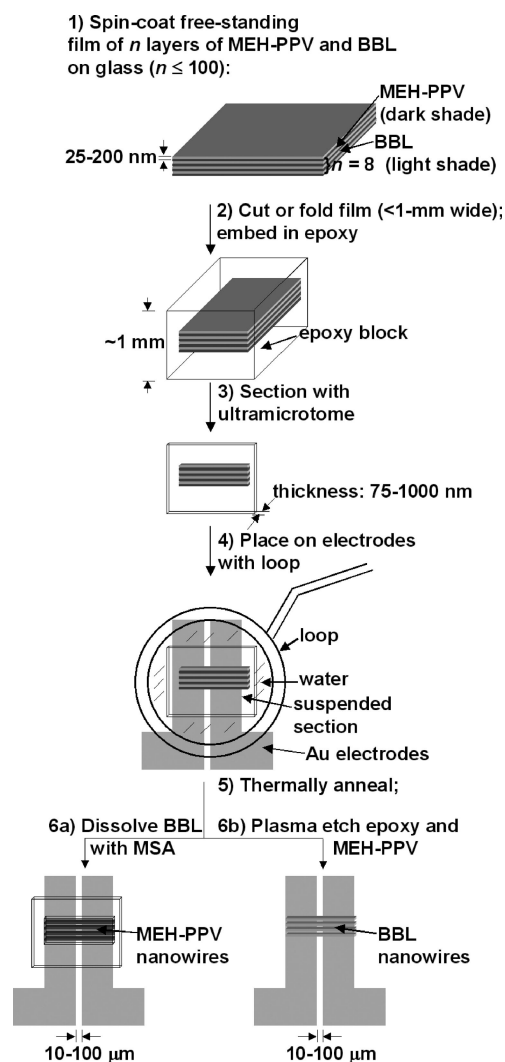


**Figure 2.** Summary of the procedure used for fabrication of multiple nanowires of MEH-PPV or BBL.

chloroform, tetrahydrofuran, and toluene). The conductivity of MEH-PPV reversibly increases several orders of magnitude upon exposure to oxidizing agents, such as I<sub>2</sub> vapor.<sup>30</sup> This feature makes it a model for monitoring the electrical response of nanowires to a chemical stimulus. It is prepared chemically by an anionic polymerization and thus is not amenable to templated electrodeposition.

BBL is a ribbon-like ladder polymer and a rare example of a conjugated polymer that exhibits high electron mobility ("n-type").<sup>31</sup> It has high tensile strength and is stable in air at high  $T$  ( $\geq 500$  °C).<sup>32</sup> Further, it is regarded as one of the most promising candidates for n-channel performance in field-effect transistors<sup>31</sup> and photovoltaic cells.<sup>33</sup> Its exclusive solubility in neat methanesulfonic acid (MSA) or highly Lewis-acidic solutions requires exhaustive aqueous rinsing of the nonvolatile MSA or decomplexation of Lewis acids from films during processing, and thus it is unlikely that any existing techniques are capable of forming nanowires of BBL.<sup>34</sup> We reasoned that, by using BBL as the sacrificial material for MEH-PPV and MEH-PPV as the sacrificial material for BBL, we could fabricate nanowires of either polymer from the same precursor film (because MEH-PPV

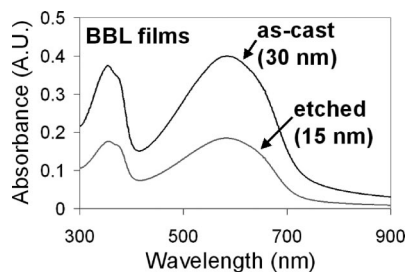


**Figure 3.** Absorption spectra of two BBL films: as-cast (30 nm) and after etching with oxygen plasma (15 nm). The absorption characteristics of the etched film changed in intensity only (decreased by one half), while it retained the features of the as-cast film.

is unaffected by MSA, and BBL is unaffected by common organic solvents and remarkably resistant to plasma etching). There are, additionally, other important potential uses of bicontinuous, densely packed nanostructures of p-type/n-type conjugated polymers, in such devices as ambipolar field-effect transistors<sup>35</sup> and photovoltaic cells.<sup>36</sup> In principle, there are many possible sacrificial materials (including photoresist or metal films) depending on the sensitivity of the conjugated polymer to the conditions required to remove the sacrificial material.

**Fabrication.** Figure 2 summarizes the procedure we used to fabricate nanowires of conjugated polymers. Spin-coating alternating layers of MEH-PPV and BBL onto glass gave a composite film (of up to 100 total layers), which we immersed in methanol, sonicated for  $\sim 5$  s and gently peeled off the substrate (step 1). (Each layer of BBL had to be immersed in water for 30 s to remove MSA and dried with a stream of  $N_2$  before deposition of the next layer of MEH-PPV.) Then, we either (i) cut  $<1$  mm wide,  $\sim 5$  mm long strips from the film with scissors or (ii) folded the film in halves  $\sim 5$  times in order to fit the entire film in a mold for embedding (step 2). A thermally curable, epoxy prepolymer (Epo-Fix, Electron Microscopy Sciences) served to embed individual strips of the film. We sectioned the cured epoxy block with an ultramicrotome (step 3), which yielded slices of the conjugated polymer film, framed by an epoxy matrix. Using a metal loop designed to suspend thin sections in a film of water by exploiting surface tension, we manually transferred the sections from the water boat of the ultramicrotome to photolithographically patterned Au electrodes on a  $SiO_2$  substrate (step 4). We controlled the position as well as the orientation of the section on the substrate using large sections that stuck reversibly to the perimeter of the metal loop, such that the section was not allowed to rotate during the transfer. Thermal annealing (at 125 °C under vacuum, step 5) improved the physical contact between the thin sections and the substrate. Selective etching of BBL with MSA (step 6a) or MEH-PPV (and epoxy) with oxygen plasma (step 6b) gave MEH-PPV or BBL nanowires, respectively.

Concern that the oxygen plasma would destroy the electronic properties of BBL led us to obtain ultraviolet–visible absorption spectra of two films: (i) as-cast and (ii) after etching (Figure 3). The as-cast film was 30 nm thick and

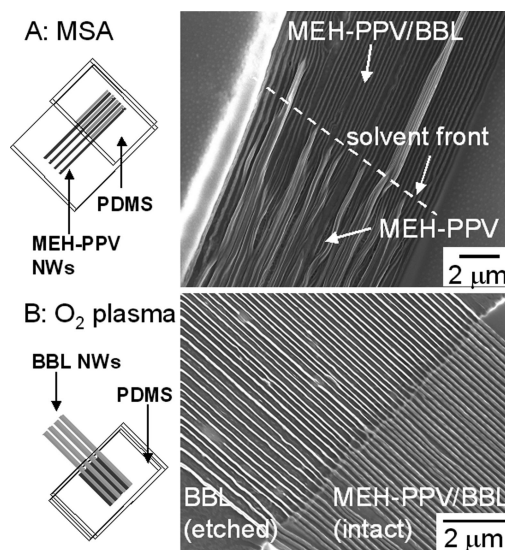


**Figure 4.** (A) Scanning electron micrograph (SEM) showing the transition between the composite MEH-PPV/BBL film and the free MEH-PPV nanowires (NWs). The image was obtained by covering a portion of the epoxy section with a conformal slab of poly(dimethylsiloxane) (PDMS) and treating the uncovered portion with a drop of methanesulfonic acid (MSA), as shown schematically on the left-hand side. The slab of PDMS was removed before acquiring the images. The solvent front is the borderline between the etched and the intact polymer film. The fibers of BBL connecting the MEH-PPV nanowires disappear after a few successive rinsings in fresh MSA. (B) Transition between the intact composite film (right-hand side) and the free BBL nanowires after dry etching of the MEH-PPV and epoxy matrix (left-hand side).

displayed an absorption spectrum consistent with previously published data.<sup>33</sup> We exposed the second film to plasma for 5 min at 1 torr and 100 W and measured a final thickness of 15 nm. The absorption intensity of the etched film decreased by one half but exhibited maxima at the same wavelengths as the as-cast film. These results suggested that the electronic structure of the bulk of BBL was unchanged by the etching step and that the oxidation of the polymer occurred only at the surface.

**Characterization of Polymer Nanowires.** Figure 4A shows the transition between the composite MEH-PPV/BBL film and the free MEH-PPV nanowires. We obtained the image by covering a portion of the epoxy section with a conformal slab of poly(dimethylsiloxane) (PDMS) and treating the uncovered portion with a drop of MSA (as shown schematically on the left-hand side of Figure 4A) for  $\sim 5$  s. We rinsed the MSA off the substrate with ethanol and removed the slab of PDMS.

Simple dissolution of MEH-PPV by its processing solvent, chloroform, did not completely remove MEH-PPV to reveal free BBL nanowires. We observed that the MEH-PPV becomes partially insoluble after spin-coating, sectioning and thermally annealing. (To use selective wet etching, a different sacrificial material would have to take the place of MEH-PPV.) Instead of wet etching, however, we chose to exploit the relative rates of dry etching by an oxygen plasma of MEH-PPV, epoxy, and BBL. We etched thin films of MEH-PPV, epoxy, and BBL in a 100 W etcher at 1 torr of ambient air and found relative rates of etching of 12:9:1 (heights



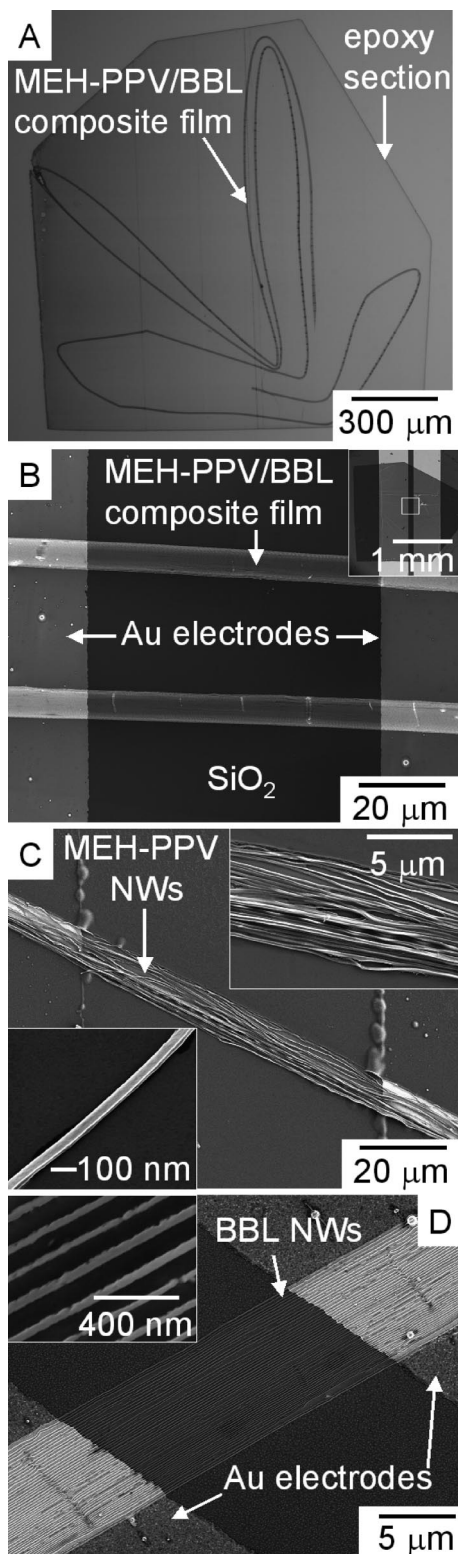


**Figure 5.** (A) Optical micrograph showing a 150 nm thick epoxy section containing a 1.5 cm long, folded, 100 layer composite film of MEH-PPV and BBL. (B) SEM of two regions of the composite film bridging Au electrodes on a SiO<sub>2</sub>/Si substrate. The inset is a global view of the epoxy slab placed over the electrodes. The white box indicates the area shown in the main image. (C) SEM of 50 MEH-PPV nanowires spanning electrodes after etching of BBL with MSA. The insets (top, right) show a close-up of the nanowires and (bottom, left) an isolated nanowire. The wires have well-defined corners and rectangular cross sections. (D) SEM of 50 BBL nanowires spanning a gap between electrodes.

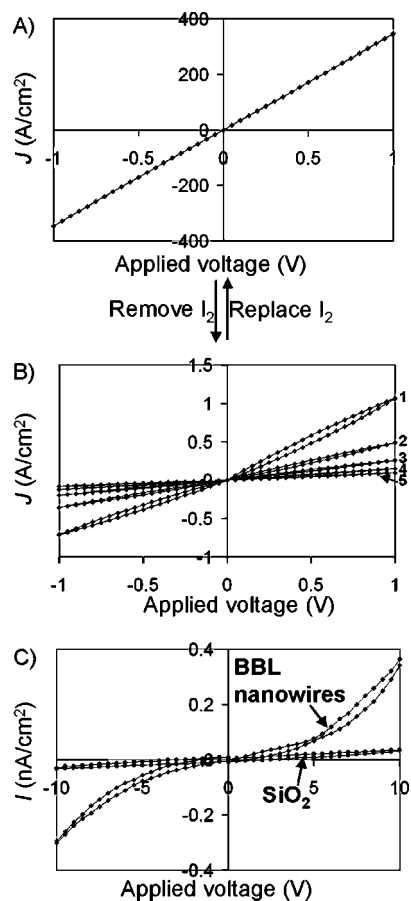


**Figure 6.** (A) Current density vs applied voltage ( $J$ - $V$ ) plot of 300 MEH-PPV nanowires in the proximity of an I<sub>2</sub> crystal. (B) The response of the same set of nanowires upon removal of the I<sub>2</sub> crystal. (C) Current vs applied voltage ( $I$ - $V$ ) of 400 BBL nanowires compared with that of the SiO<sub>2</sub> substrate.

measured by profilometry). Figure 4B shows the transition between the intact composite film (right-hand side) and the free BBL nanowires after dry etching of the MEH-PPV and epoxy matrix (left-hand side).

**Nanowires Bridging Electrodes.** We obtained sections like the one shown in the optical image of Figure 5A. The epoxy sections contained a  $\sim 1.5$  cm long, 100 layer film of MEH-PPV and BBL and were 150 or 200 nm thick. We folded the film in order to ensure that it would span a set of parallel electrodes no matter what orientation we deposited the epoxy slab.<sup>37</sup> Figure 5B shows an SEM image of two regions of the folded composite film over Au electrodes (the gap is 50  $\mu$ m). The epoxy section that contains the composite film is “transparent” because we obtained the image at a relatively high accelerating voltage (5 kV). The inset shows a global view of the section over electrodes; the white box indicates the region shown in the main image.

Figure 5C shows uniaxially aligned MEH-PPV nanowires, after wet etching of BBL, spanning electrodes. This image was acquired at 2 kV, so the surrounding epoxy is “opaque” and clearly visible. The insets are of a group of nanowires (top right) and an isolated nanowire (bottom left). The edges of each individual nanowire are sharp, and the nanowires have the expected rectangular cross sections. The MEH-PPV nanowires have a tendency to aggregate, due to capillary

forces, while the rinsing solvent, ethanol, evaporates. Figure 5D shows BBL nanowires spanning a 25  $\mu\text{m}$  gap between electrodes after dry etching the MEH-PPV layers and the epoxy matrix.

**Application to Sensing by Reversible Doping.**  $\text{I}_2$  reversibly increases the conductivity of many conjugated polymers by several orders of magnitude.<sup>28</sup> We measured the electrical response of a group of 300 MEH-PPV nanowires (cross section: 200 nm  $\times$  100 nm, each) to  $\text{I}_2$  vapor by placing a crystal of solid  $\text{I}_2$  about 2 mm from the nanowires.<sup>38</sup> Three successive cycles of applied voltage (0 V  $\rightarrow$  1 V  $\rightarrow$  -1 V  $\rightarrow$  0 V) yielded overlapping plots and no hysteresis (Figure 6A). Upon removal of the  $\text{I}_2$ , we observed a decrease in current density by a factor of  $10^3$  in the time it took to remove the  $\text{I}_2$  and obtain another measurement ( $\sim 10$  s; see Figure 6B). The conductivity continued to decrease over five consecutive cycles of applied voltage (labeled 1 through 5 in Figure 6B; the experiment lasted 135 s total). We attribute the loss of conductivity to the loss of  $\text{I}_2$  from the MEH-PPV nanowires and a concomitant decrease in the density of charge carriers in the material. When we replaced the  $\text{I}_2$  near the wires, the MEH-PPV nanowires recovered the original conductivity of Figure 6A. From the current density versus applied voltage ( $J$ - $V$ ) data for this representative group of nanowires, we calculated an approximate conductivity of 4 S  $\text{cm}^{-1}$  (approximate because the orientation of the nanowires was not always exactly perpendicular to the electrodes). Our value for doped conductivity is reasonable for a doped film of MEH-PPV.<sup>30</sup>

Although BBL is not sensitive to oxidants such as  $\text{I}_2$ , we were able to distinguish pairs of electrodes that were spanned by BBL nanowires from those that were not. Figure 6C is a current versus voltage ( $I$ - $V$ ) plot; we attribute the conductivity to a set of 400 BBL nanowires that spans the 50  $\mu\text{m}$  gap between the electrodes. The second plot in Figure 6C ("SiO<sub>2</sub>") is a hysteretic curve of a pair of electrodes that are not spanned by nanowires. It displays much lower conductance, characteristic of conductivity across the bare SiO<sub>2</sub> substrate. In the linear region in the center of the BBL curve, we calculated an approximate conductivity of  $10^{-6}$  S  $\text{cm}^{-1}$ . The conductivity of BBL is a strong function of its processing history and ranges over 14 orders of magnitude in the literature:  $10^{-14}$  to  $10^{-12}$  S  $\text{cm}^{-1}$  for pristine films,<sup>39</sup>  $10^{-6}$  S  $\text{cm}^{-1}$  for annealed films,<sup>40</sup> and  $10^0$  S  $\text{cm}^{-1}$  for p-type-doped films (AsF<sub>5</sub>).<sup>40</sup> Residual MEH-PPV could not have been responsible for the conductivity, because at the end of the etching step, the junction no longer responded to  $\text{I}_2$ . The shape of the  $I$ - $V$  plot shown in Figure 6C for BBL nanowires is consistent with those of thin films that we have measured.

In conclusion, we have developed a general technique for the fabrication of conjugated polymer nanowires. We believe that this technique is at least as simple, conceptually and operationally, as any existing method. It has the potential to replace other techniques in many circumstances, particularly where sophisticated processes such as electron-beam lithography are not available and when relatively small lengths (<1 mm) of nanostructured material are required. We are unaware of a film-forming conjugated polymer that, in

principle, cannot be made into nanowires by this method. It should be possible to select sacrificial materials that have orthogonal processing conditions (e.g., rates of wet or dry etching) to many conjugated polymers of interest. The entire process, from spin-coating to electrical characterization, can be executed in a single day and does not require access to a cleanroom. We believe that nanoskiving can address some of the limitations of current techniques for the fabrication of conjugated polymer nanostructures, and that it will enable new architectures that have been otherwise difficult to obtain.

**Acknowledgment.** This work was supported by the National Science Foundation under award CHE-0518055. The authors used the shared facilities supported by the NSF under NSEC (PHY-0117795 and PHY-0646094) and MR-SEC (DMR-0213805). This work was performed in part using the facilities of the Center for Nanoscale Systems (CNS), a member of the National Nanotechnology Infrastructure Network (NNIN), which is supported by the National Science Foundation under NSF Award No. ECS-0335765. CNS is part of the Faculty of Arts and Sciences at Harvard University. The authors thank Dr. Richard Schalek for training on the ultramicrotome.

**Supporting Information Available:** Detail of the fabrication process. This information is available free of charge via the Internet at <http://pubs.acs.org>.

## References

- (1) Xu, Q. B.; Bao, J. M.; Capasso, F.; Whitesides, G. M. *Angew. Chem., Int. Ed.* **2006**, *45*, 3631–3635.
- (2) Xu, Q. B.; Gates, B. D.; Whitesides, G. M. *J. Am. Chem. Soc.* **2004**, *126*, 1332–1333.
- (3) Xu, Q. B.; Perez-Castillejos, R.; Li, Z. F.; Whitesides, G. M. *Nano Lett.* **2006**, *6*, 2163–2165.
- (4) Xu, Q. B.; Rioux, R. M.; Whitesides, G. M. *ACS Nano* **2007**, *1*, 215227.
- (5) Xu, Q. B.; Bao, J. M.; Rioux, R. M.; Perez-Castillejos, R.; Capasso, F.; Whitesides, G. M. *Nano Lett.* **2007**, *7*, 2800–2805.
- (6) Liu, H. Q.; Kameoka, J.; Czaplewski, D. A.; Craighead, H. G. *Nano Lett.* **2004**, *4*, 671–675.
- (7) Hernandez, S. C.; Chaudhuri, D.; Chen, W.; Myung, N. V.; Mulchandani, A. *Electroanalysis* **2007**, *19*, 2125–2130.
- (8) Ramanathan, K.; Bangar, M. A.; Yun, M.; Chen, W.; Myung, N. V.; Mulchandani, A. *J. Am. Chem. Soc.* **2005**, *127*, 496–497.
- (9) Wanekaya, A. K.; Chen, W.; Myung, N. V.; Mulchandani, A. *Electroanalysis* **2006**, *18*, 533–550.
- (10) Wanekaya, A. K.; Bangar, M. A.; Yun, M.; Chen, W.; Myung, N. V.; Mulchandani, A. *J. Phys. Chem. C* **2007**, *111*, 5218–5221.
- (11) Liu, H. Q.; Reccius, C. H.; Craighead, H. G. *Appl. Phys. Lett.* **2005**, *87*.
- (12) Samitsu, S.; Shimomura, T.; Ito, K.; Fujimori, M.; Heike, S.; Hashizume, T. *Appl. Phys. Lett.* **2005**, *86*.
- (13) He, H. X.; Li, C. Z.; Tao, N. J. *Appl. Phys. Lett.* **2001**, *78*, 811–813.
- (14) Sirringhaus, H.; Tessler, N.; Friend, R. H. *Science* **1998**, *280*, 1741–1744.
- (15) Yu, G.; Gao, J.; Hummelen, J. C.; Wudl, F.; Heeger, A. J. *Science* **1995**, *270*, 1789–1791.
- (16) Sirringhaus, H.; Brown, P. J.; Friend, R. H.; Nielsen, M. M.; Bechgaard, K.; Langeveld-Voss, B. M. W.; Spiering, A. J. H.; Janssen, R. A. J.; Meijer, E. W.; Herwig, P.; de Leeuw, D. M. *Nature* **1999**, *401*, 685–688.
- (17) Chiang, C. K.; Fincher, C. R.; Park, Y. W.; Heeger, A. J.; Shirakawa, H.; Louis, E. J.; Gau, S. C.; MacDiarmid, A. G. *Phys. Rev. Lett.* **1977**, *39*, 1098–1101.
- (18) Menard, E.; Meitl, M. A.; Sun, Y. G.; Park, J. U.; Shir, D. J. L.; Nam, Y. S.; Jeon, S.; Rogers, J. A. *Chem. Rev.* **2007**, *107*, 1117–1160.
- (19) Cui, Y.; Wei, Q. Q.; Park, H. K.; Lieber, C. M. *Science* **2001**, *293*, 1289–1292.

- (20) McQuade, D. T.; Pullen, A. E.; Swager, T. M. *Chem. Rev.* **2000**, *100*, 2537–2574.
- (21) Duvail, J. L.; Retho, P.; Fernandez, V.; Louarn, G.; Molinie, P.; Chauvet, O. *J. Phys. Chem. B* **2004**, *108*, 18552–18556.
- (22) Smela, E. *Adv. Mater.* **2003**, *15*, 481–494.
- (23) Yun, M. H.; Myung, N. V.; Vasquez, R. P.; Lee, C. S.; Menke, E.; Penner, R. M. *Nano Lett.* **2004**, *4*, 419422.
- (24) Kameoka, J.; Czaplewski, D.; Liu, H. Q.; Craighead, H. G. *J. Mater. Chem.* **2004**, *14*, 1503–1505.
- (25) Li, D.; Babel, A.; Jenekhe, S. A.; Xia, Y. N. *Adv. Mater.* **2004**, *16*, 2062–2066.
- (26) McCann, J. T.; Chen, J. I. L.; Li, D.; Ye, Z. G.; Xia, Y. N. *Chem. Phys. Lett.* **2006**, *424*, 162–166.
- (27) Dong, B.; Lu, N.; Zelsmann, M.; Kehagias, N.; Fuchs, H.; Torres, C. M. S.; Chi, L. F. *Adv. Funct. Mater.* **2006**, *16*, 1937–1942.
- (28) Lim, J. H.; Mirkin, C. A. *Adv. Mater.* **2002**, *14*, 1474–1477.
- (29) Gates, B. D.; Xu, Q. B.; Stewart, M.; Ryan, D.; Willson, C. G.; Whitesides, G. M. *Chem. Rev.* **2005**, *105*, 1171–1196.
- (30) Wudl, F.; Srdanov, G. Conducting Polymer Formed Of Poly(2-methoxy,5-(2'-ethylhexyloxy)-p-phenylenevinylene. United States Patent 5,189,136.
- (31) Babel, A.; Jenekhe, S. A. *J. Am. Chem. Soc.* **2003**, *125*, 13656–13657.
- (32) Arnold, F. E.; Vandeuse, R. *Macromolecules* **1969**, *2*, 497–&.
- (33) Alam, M. M.; Jenekhe, S. A. *Chem. Mater.* **2004**, *16*, 4647–4656.
- (34) Roberts, M. F.; Jenekhe, S. A. *Polymer* **1994**, *35*, 4313–4325.
- (35) Babel, A.; Zhu, Y.; Cheng, K. F.; Chen, W. C.; Jenekhe, S. A. *Adv. Funct. Mater.* **2007**, *17*, 2542–2549.
- (36) Halls, J. J. M.; Walsh, C. A.; Greenham, N. C.; Marseglia, E. A.; Friend, R. H.; Moratti, S. C.; Holmes, A. B. *Nature* **1995**, *376*, 498–500.
- (37) Alternatively, we have used epoxy blocks that contain individual strips of the composite film that, after sectioning, we addressed electrically with evaporated top contacts through a stencil mask.
- (38) We note that our two-point measurement does not decouple contact resistance from material resistance. To determine the contribution of contact resistance, a four-point measurement would be required (see ref. 6).
- (39) Alam, M. M.; Jenekhe, S. A. *J. Phys. Chem. B* **2002**, *106*, 11172–11177.
- (40) Coter, F.; Belaish, Y.; Davidov, D.; Dalton, L. R.; Ehrenfreund, E.; McLean, M. R.; Nalwa, H. S. *Synth. Met.* **1989**, *29*, E471–E476.

NL8009318